Journal Pre-proof



Occlusal Surface Accuracy of Milled and DLP-Printed Complete Denture Teeth: Effects of Arch Segmentation and Tooth-Set Size

Mehmet Buğra Türkcan, Erdal Eroğlu, Kadir Kıran

PII: S2950-6433(26)00071-1

DOI: https://doi.org/10.1016/j.ddj.2026.100137

Reference: DDJ 100137

To appear in: *Digital Dentistry Journal*

Received Date: 30 September 2026

Revised Date: 28 October 2026

Accepted Date: 3 November 2026

Please cite this article as: M.B. Türkcan, E. Eroğlu, K. Kıran, Occlusal Surface Accuracy of Milled and DLP-Printed Complete Denture Teeth: Effects of Arch Segmentation and Tooth-Set Size, *Digital Dentistry Journal*, https://doi.org/10.1016/j.ddj.2026.100137.

This is a PDF of an article that has undergone enhancements after acceptance, such as the addition of a cover page and metadata, and formatting for readability. This version will undergo additional copyediting, typesetting and review before it is published in its final form. As such, this version is no longer the Accepted Manuscript, but it is not yet the definitive Version of Record; we are providing this early version to give early visibility of the article. Please note that Elsevier's sharing policy for the Published Journal Article applies to this version, see: https://www.elsevier.com/about/policies-and-standards/sharing#4-published-journal-article. Please also note that, during the production process, errors may be discovered which could affect the content, and all legal disclaimers that apply to the journal pertain.

© 2026 Published by Elsevier Ltd.

Journal Pre-proof

TITLE PAGE

Occlusal Surface Accuracy of Milled and DLP-Printed Complete Denture Teeth: Effects of Arch Segmentation and Tooth-Set Size

Full Length Article

Authors

[Mehmet Buğra Türkcan] [a]; [Erdal Eroğlu] [a]; [Kadir Kıran] [b, c]

Affiliations

[a] [Süleyman Demirel University Faculty of Dentistry, Department of Prosthodontics, Isparta, Türkiye]

[b] [Süleyman Demirel University, School of Civil Aviation, Department of Aircraft Maintenance and Repair, Isparta, Türkiye]

[c] [Süleyman Demirel University, Innovative Technologies Application and Research Center, Isparta, Türkiye]

Corresponding author

[Mehmet Buğra Türkcan]
[Süleyman Demirel University Faculty of Dentistry, Department of Prosthodontics, Isparta, Türkiye]
Email: [mehmetturkcan@sdu.edu.tr]

Declaration of competing interests

[The authors declare that they have no known competing financial interests or personal relationships that could have appeared to influence the work reported in this paper.]

Funding

[This research received no specific grant from funding agencies in the public, commercial, or not-for-profit sectors.]

CRediT author statement

[**Mehmet Buğra Türkcan**: Writing – review & editing, Writing – original draft, Visualization, Validation, Resources, Methodology, Investigation, Formal analysis, Data curation. **Erdal Eroğlu**: Writing – review & editing, Writing – original draft, Validation, Supervision, Re sources, Project administration, Methodology, Investigation, Formal analysis, Data curation, Conceptualization**. Kadir Kıran**: Writing – re view & editing, Validation, Software, Resources, Formal analysis.]

Journal Pre-proof

Journal Pre-proof

Occlusal Surface Accuracy of Milled and DLP-Printed Complete Denture Teeth: Effects of Arch Segmentation and Tooth-Set Size

Abstract

Objective

This in vitro study evaluated the effects of manufacturing method, one-piece or three-segment configuration, and tooth-set size on the occlusal surface morphology of complete denture teeth relative to the reference computer-aided design (CAD) model.

Materials and Methods

Eighty-four maxillary tooth arches were fabricated in a balanced 2 × 2 × 3 factorial design (n = 7): digital light processing (DLP) or milling; one-piece or three-segment fabrication; and small, medium, or large tooth sets. Technology-specific photopolymer resin and prepolymerized polymethyl methacrylate (PMMA) systems were used. Occlusal evaluation regions were predefined on the reference CAD geometry. One-piece arches were aligned as a whole and segments independently to their corresponding reference regions using best-fit registration. Root mean square (RMS) deviations were calculated in millimeters; segment values were combined using an equal-weight quadratic mean. Data were analyzed using three-way analysis of variance and Bonferroni-adjusted comparisons.

Results

Overall mean RMS values were 0.0713 ± 0.0208 mm for DLP and 0.1040 ± 0.0176 mm for milling, and 0.0746 ± 0.0220 mm for three-segment and 0.1007 ± 0.0214 mm for one-piece fabrication. DLP and segmentation had lower RMS within corresponding subgroups, and RMS increased with tooth size (Bonferroni-adjusted $p < 0.001$). The three-way interaction was significant ($p = 0.001$); the method × tooth size interaction was not.

Conclusions

The factorial comparison provides quantitative data for developing the tested manufacturing protocols to reproduce CAD-defined occlusal morphology. Independent segment alignment excludes assembly-related positional errors. The small RMS differences may have negligible clinical impact in vivo, requiring validation of bonded assemblies before recommending routine three-segment fabrication.

Introduction

Complete edentulism remains an important oral health problem because it can adversely affect mastication, speech, esthetics, and quality of life [1,2]. Computer-aided design and computer-aided manufacturing (CAD/CAM) technologies have expanded treatment options for complete dentures by enabling digital design, reproducible fabrication, and storage of prosthetic data [3,4]. Digital complete dentures can be fabricated using either subtractive manufacturing, in which a prepolymerized material is milled, or additive manufacturing, in which a photopolymer material is built layer by layer [5-7].

The manufacturing accuracy of a digital prosthesis is not determined solely by the fabrication technology employed. The CAD/CAM system, material, fabricated geometry, and evaluation protocol may also influence accuracy [5]. This is particularly relevant for complete denture teeth. Occlusal surfaces contain cusps, fossae, grooves, marginal ridges, and narrow transitional

regions, and reproducing these intricate features with milling burs may be challenging. Additive manufacturing, in contrast, can be influenced by printing orientation, layer-by-layer polymerization, support placement, washing procedures, and post-polymerization protocols [6,7]. Previous studies have shown that the geometric accuracy of denture teeth may vary according to tooth type and manufacturing approach [8,9], and that design-related variables may affect the occlusal accuracy of 3D-printed complete dentures [10].

Contemporary complete denture CAD software allows tooth libraries to be selected in different sizes and dental arches to be fabricated as one connected structure or smaller segments. These choices alter geometry and volume and may influence cumulative dimensional changes in additive manufacturing and bur accessibility and toolpaths in milling. Although the accuracy of denture bases and complete dentures has been investigated extensively [5,11,12], the combined effects of manufacturing method, segmentation, and tooth-set size on occlusal surface reproduction remain unclear. Joint assessment can provide manufacturing benchmarks and identify interactions relevant to protocol development.

This in vitro study aimed to compare the occlusal surface geometric accuracy of small, medium, and large complete denture tooth sets manufactured by DLP or milling as either one-piece or three-segment configurations. Four null hypotheses were tested: (H01) the manufacturing method would have no effect on RMS deviation; (H02) the manufacturing configuration would have no effect on RMS deviation; (H03) tooth size would have no effect on RMS deviation; and (H04) there would be no two-way or three-way interactions among manufacturing method, manufacturing configuration, and tooth size.

Materials and Methods

Study Design and Sample Size

This in vitro study used a balanced 2 × 2 × 3 factorial design. The investigated factors were manufacturing method (DLP additive manufacturing or milling), manufacturing configuration (i.e., integrated one-piece or segmented), and tooth size (i.e., small, medium, or large). The primary outcome variable was the three-dimensional geometric deviation of the predefined functional occlusal surface relative to the corresponding CAD reference, expressed as root mean square (RMS). The study did not aim to evaluate the absolute positional accuracy of the teeth within the denture base or dental arch, but rather to determine the extent to which the occlusal surface morphology reproduced the reference design after manufacturing.

An a priori sample size calculation was performed using G*Power 3.1.9.7, with the F tests family and the “ANOVA: Fixed effects, special, main effects and interactions” option. The effect-size value of 0.419 reported by Namano et al. [13] was adopted directly and entered as Cohen’s f, without recalculation or conversion from their published results. Its application to the present three-way interaction was treated as a literature-based planning assumption. Namano et al. did not report the specific pilot outcome or comparison used to obtain this value or the numerical procedure by which it was derived. The calculation targeted the manufacturing method × manufacturing configuration × tooth size interaction, with numerator degrees of freedom of 2, 12 experimental cells, $\alpha = 0.05$, and a target power of 0.90. The experimental unit was the maxillary dental arch. The minimum required total sample size was 76. To maintain equal allocation across the balanced 2 × 2 × 3 factorial design, 84 specimens were included, with seven specimens per experimental cell. Under the assumed effect size of $f = 0.419$, the

calculated power at N = 84 was approximately 93%. Ethics committee approval was not required because no patient data, patient records, or biological materials were used.

Reference Design and Experimental Groups

After calibrating the CEDU 3D QScanner Pro laboratory scanner (CEDU Technology, Hangzhou, China), we digitized a maxillary edentulous model (Frasaco B-3 NH, Germany). The resulting STL file was imported into exocad software (exocad GmbH, Germany), and a maxillary complete denture design was created using the complete denture module. We used the Generic Lingualize tooth library to generate small (S), medium (M), and large (L) tooth sets.

To quantitatively demonstrate geometric size differences among the CAD designs, we calculated STL volumes using Geomagic Control X 2020 software (3D Systems, South Carolina, USA). The total volumes of the integrated one-piece and segmented designs were 3315.43 mm^3 and 3305.76 mm^3, respectively, for the S group; 4182.59 mm^3 and 4186.51 mm^3 for the M group; and 4988.88 mm^3 and 4986.64 mm^3 for the L group. Thus, geometric volume increased progressively from S to L, whereas the total volumes of the integrated one-piece and segmented designs for the same tooth size remained comparable.

For the integrated one-piece specimens, the entire maxillary complete denture tooth arch was manufactured as a single connected structure. For the segmented specimens, the tooth arch was divided into three components: an anterior segment extending from canine to canine, a right posterior segment comprising connected premolar and molar teeth, and a corresponding left posterior segment. We considered these three segments components of the same experimental specimen rather than independent observations. Because additive and subtractive manufacturing technologies use different fabrication mechanisms, each workflow used a material system compatible with its respective manufacturing principle.

The three-segment configuration provided an experimental comparison between a continuous arch and shorter, anatomically defined structures while retaining connected teeth within each region. This comparison addressed a manufacturing design variable; it did not constitute validation of a clinical assembly protocol.

The specimens were produced across multiple manufacturing batches, discs, and manufacturing sessions until the target sample size was reached. The criteria for identifying defective specimens were established before fabrication and included incomplete fabrication, fracture or deformation during support removal, and visible fabrication-related surface defects, including surface discontinuities associated with printing or milling. Following manufacturing and before deviation analysis, specimens were visually inspected by comparison with the reference model. When a defect was identified, the affected component was remanufactured in a separate session while maintaining the same printing or milling parameters. Only specimens meeting the visual acceptance criteria proceeded to deviation analysis. The number and group distribution of remanufactured components were not prospectively recorded and could not be reconstructed retrospectively.

Subtractive Manufacturing

The STL files were imported into MillBox CAM software (CIMsystem, Italy), positioned within the PMMA discs, and processed to generate connector positions and milling toolpaths. Complete denture teeth were fabricated by dry milling using a five-axis M20 milling unit

(CamCube, Montreal, Canada), prepolymerized PMMA discs measuring 98 mm in diameter and 18 mm in thickness (Bilkim Kimya Sanayi, İzmir, Türkiye), and 1.0- and 2.0-mm milling burs. The spindle speed and feed rate values were not available for reporting. After milling, the specimens were separated from the discs, the connectors were removed, and the surfaces were visually inspected without altering the anatomical morphology (Figure 1).

We used the milled denture bases solely as standardized carriers during scanning. We evaluated each tooth-size and manufacturing-configuration group on its corresponding carrier denture base. We did not include denture base surfaces in the alignment or deviation analyses.

Additive Manufacturing

For DLP manufacturing, the STL files were imported into DentaFab Slicer software (DentaFab, İstanbul, Türkiye). The integrated one-piece and segmented designs were prepared separately and oriented using rotations of 180° about the X axis and 0° about the Y axis. The same orientation settings were used in every DLP manufacturing run. Supports were generated automatically, with a support spacing of 2 mm. At this orientation, supports were placed exclusively on the apical surfaces, and no supports were placed on the functional occlusal surfaces. The layer thickness was set to 50 µm. The specimens were manufactured using Power Resins C&B Ceramic Resin (DentaFAB, İstanbul, Türkiye) and a DentaFAB Sega DLP printer (DentaFAB, İstanbul, Türkiye).

After manufacturing, the specimens were washed in 96% ethanol for 3 minutes; the solution was replaced, and a second 3-minute washing cycle was performed. The supports were removed using side cutters, and the specimens underwent post-polymerization for 15 minutes in a FastCure light-curing unit (CamCube, Montreal, Canada). The completed specimens were visually inspected for surface integrity and manufacturing defects (Figure 2).

Scanning, Alignment, and 3D Deviation Analysis

Each integrated one-piece dental arch was scanned once to generate a single STL file. For segmented specimens, each of the three constituent segments was scanned once, generating three separate STL files per arch. No repeated scans of the same arch or segment were performed. All scanning procedures, best-fit alignments, and RMS analyses in Geomagic Control X 2020 were performed by a single operator. The scanner was calibrated before scanning each experimental group of seven arch-level specimens. For segmented groups, each of these seven specimens comprised three separately scanned segments.

The integrated one-piece specimens were positioned on their corresponding carrier denture bases and scanned using the same laboratory scanner. For the segmented specimens, each of the three segments was positioned and scanned separately to allow direct comparison with its corresponding reference geometry. Before scanning, we verified complete seating of each specimen on the denture base and applied the same positioning protocol to all groups. The segmented specimens were scanned separately to enable direct comparison of each segment's occlusal surface geometry with the corresponding reference region, rather than to assess positional accuracy within the arch.

We defined the functional occlusal evaluation region once on the reference CAD model before analysis, and it remained unchanged throughout all measurements. This region comprised the functional occlusal surfaces, including cusp tips, occlusal ridges, fossae, grooves, and marginal ridges. We excluded cervical, basal, and other nonocclusal surfaces from the analysis. We

applied the same anatomical boundary criteria to all the reference STL geometries; while the test specimens varied, the reference evaluation surface remained unchanged. For the segmented specimens, we evaluated the anterior, right posterior, and left posterior segments against their corresponding predefined occlusal regions of the fixed reference design.

The reference and test STL files were imported into Geomagic Control X 2020 software. Because positional accuracy was outside the scope of the study, we intentionally minimized rigid-body translational and rotational differences between the manufactured specimens and the reference design using best-fit alignment [14,15]. The analysis therefore focused on the accuracy of the predefined occlusal surface geometry relative to the reference design. After alignment, we calculated three-dimensional surface deviations and recorded RMS values in millimeters. A lower RMS value indicated a smaller geometric deviation from the reference occlusal surface (Figure 3). Each one-piece arch underwent one common rigid-body alignment, whereas each of the three segments underwent its own alignment. Consequently, the relative positions of the segments were not retained in the combined RMS outcome. A completed, bonded three-segment denture was not evaluated as a single assembled unit.

For segmented specimens, separate RMS values were obtained for the anterior, right posterior, and left posterior segments. Because these segments constituted a single experimental arch, their RMS values were combined into one arch-level outcome using an equal-weight quadratic mean [16] (Figure 4). Specifically, the three segment RMS values were squared, averaged with equal weights, and then square-rooted. Equal weighting was selected to give each predefined anatomical segment an equal contribution to the composite outcome, rather than determining its contribution according to its surface area or number of sampled points. Thus, larger or more densely sampled segments were not assigned greater weight in the aggregation. The resulting value represents an equally weighted composite of segment-level deviations, expressed in millimeters, rather than a pooled RMS calculated across all surface points. The implications of this weighting choice are acknowledged in the Discussion.

We generated 3D color-coded deviation maps for visual assessment. Following the protocol used in the reference study, we set the nominal and critical limits for the color-coded deviation maps at ±100 μm and ±500 μm, respectively [17] (Figures 5 and 6). These limits were used for visualization and were not treated as validated thresholds for clinical acceptability.

Statistical Analysis

We performed statistical analyses using IBM SPSS Statistics 22 (IBM Corp., Armonk, NY, USA). We assessed distributional characteristics within the factor groups using skewness and kurtosis values, histograms, and Q-Q plots, and evaluated homogeneity of variances using Levene's test. The primary inferential analysis was a three-way factorial analysis of variance (ANOVA), with manufacturing method, manufacturing configuration, and tooth size entered as fixed factors and all two-way and three-way interactions included in the model.

After detecting a significant three-way interaction, we performed simple effects and simple-simple effects comparisons to evaluate differences within specific factor levels. Bonferroni adjustment was applied for multiple comparisons. When a significant higher-order interaction was present, these marginal comparisons were not interpreted as independent effects. Statistical significance was set at $\alpha = 0.05$.

Results

Distribution Assessment and Simple-Effects Comparisons

Skewness values within ±2.0 and kurtosis values within ±7.0 across all factor groups supported parametric analyses. Visual inspection of the residual Q-Q plots and residual-versus-predicted value plots indicated no substantial violations of the assumptions of normality or homogeneity of variance. Homogeneity of variance was satisfied across the 12 experimental cells (Levene's $F = 0.307$; $p = 0.737$).

In the Bonferroni-adjusted simple-effects comparisons, all pairwise comparisons among tooth sizes were significant within each manufacturing method × manufacturing configuration combination, with RMS values increasing progressively from small to large tooth sets (a-c; $p < 0.001$). Within each manufacturing method × tooth size combination, segmented manufacturing resulted in significantly lower RMS values than integrated one-piece fabrication (A-B; $p < 0.001$). Likewise, within the same manufacturing configuration × tooth size conditions, specimens manufactured using DLP exhibited significantly lower RMS values than those in the milling group (x-y; $p < 0.001$). The lowest mean RMS value was observed in the small, segmented DLP group (0.0443 ± 0.0023 mm), whereas the highest was observed in the large, integrated one-piece milling group (0.1371 ± 0.0061 mm) (Table 1, Figure 7).

Based on the rounded group means in Table 1, the one-piece minus segmented differences in mean RMS ranged from 0.0131 to 0.0319 mm for milling and from 0.0247 to 0.0368 mm for DLP. The milling minus DLP differences ranged from 0.0202 to 0.0405 mm within corresponding manufacturing configuration × tooth size combinations. These values describe differences between RMS outcomes rather than direct measurements of tooth displacement.

Table 1. RMS values (mm) according to manufacturing method, manufacturing configuration, and tooth size, with Bonferroni-adjusted simple-effects comparisons.

Manufacturing method	Tooth size	Manufacturing configuration	n	RMS (mm), Mean ± SD
Milling	Small	Integrated one-piece	7	0.0961^{aAx} ± 0.0038
Milling	Small	Segmented	7	0.0830^{aBx} ± 0.0032
Milling	Medium	Integrated one-piece	7	0.1089^{bAx} ± 0.0044
Milling	Medium	Segmented	7	0.0939^{bBx} ± 0.0016
Milling	Large	Integrated one-piece	7	0.1371^{cAx} ± 0.0061
Milling	Large	Segmented	7	0.1052^{cBx} ± 0.0049
DLP	Small	Integrated one-piece	7	0.0690^{aAy} ± 0.0039
DLP	Small	Segmented	7	0.0443^{aBy} ± 0.0023
DLP	Medium	Integrated one-piece	7	0.0887^{bAy} ± 0.0039
DLP	Medium	Segmented	7	0.0534^{bBy} ± 0.0013

Manufacturing method	Tooth size	Manufacturing configuration	n	RMS (mm), Mean ± SD
DLP	Large	Integrated one-piece	7	$0.1045^{cAy} \pm 0.0038$
DLP	Large	Segmented	7	$0.0677^{cBy} \pm 0.0029$

DLP, digital light processing; n, number of specimens; RMS, root mean square; SD, standard deviation. RMS values are expressed in millimeters. Different lowercase letters (a-c) indicate Bonferroni-adjusted significant differences among tooth sizes within the same manufacturing method and manufacturing configuration; different uppercase letters (A-B) indicate significant differences between manufacturing configurations within the same manufacturing method and tooth size; and different letters x-y indicate significant differences between manufacturing methods within the same manufacturing configuration and tooth size ($p < 0.001$). Letter annotations should be interpreted only within the specified subgroup comparisons. One-piece RMS values were obtained after arch-level registration; segmented values are equal-weight composites after independent registration of the three segments and do not assess the positional accuracy of a bonded assembly.

Three-way ANOVA

The overall three-way ANOVA model was statistically significant ($F(11, 72) = 337.502$; $p < 0.001$) and explained 98.1% of the variance in RMS values ($R^2 = 0.981$; adjusted $R^2 = 0.978$). Significant main effects were observed for manufacturing method ($F = 1610.350$; $p < 0.001$; partial $\eta^2 = 0.957$), manufacturing configuration ($F = 1024.487$; $p < 0.001$; partial $\eta^2 = 0.934$), and tooth size ($F = 470.116$; $p < 0.001$; partial $\eta^2 = 0.929$).

Among the two-way interactions, the manufacturing method × manufacturing configuration interaction ($F = 56.349$; $p < 0.001$; partial $\eta^2 = 0.439$) and the tooth size × manufacturing configuration interaction ($F = 30.315$; $p < 0.001$; partial $\eta^2 = 0.457$) were statistically significant. In contrast, the manufacturing method × tooth size interaction was not statistically significant ($F = 2.760$; $p = 0.070$; partial $\eta^2 = 0.071$). The manufacturing method × manufacturing configuration × tooth size three-way interaction was also significant ($F = 7.479$; $p = 0.001$; partial $\eta^2 = 0.172$) (Table 2).

The significant three-way interaction indicated that the effect of one factor on RMS deviation varied depending on the levels of the other two factors. Therefore, we did not interpret the main effects in isolation; instead, we based our interpretation primarily on the Bonferroni-adjusted simple-effects comparisons.

Table 2. Three-way ANOVA results for RMS deviation (mm).

Effect	df	F	p	Partial η^2
Manufacturing method	1	1610.350	<0.001	0.957
Manufacturing configuration	1	1024.487	<0.001	0.934
Tooth size	2	470.116	<0.001	0.929
Manufacturing method × tooth size	2	2.760	0.070	0.071
Manufacturing method × manufacturing configuration	1	56.349	<0.001	0.439
Tooth size × manufacturing configuration	2	30.315	<0.001	0.457
Manufacturing method × manufacturing configuration × tooth size	2	7.479	0.001	0.172

Error df = 72. Partial η^2: partial eta squared.

Discussion

By jointly evaluating manufacturing method, manufacturing configuration, and tooth-set size in 84 maxillary tooth arches, this study quantified how these variables were associated with the reproduction of CAD-defined occlusal morphology. The balanced 12-cell factorial design enabled their interactions to be examined within one experimental framework, using predefined occlusal reference regions. H01, H02, and H03 were rejected. Because the manufacturing method × manufacturing configuration, tooth size × manufacturing configuration, and three-way interactions were significant, whereas the manufacturing method × tooth size interaction was not, H04 was also rejected. The significant three-way interaction shows that the magnitude of the differences depended on the combination of factors, making the subgroup comparisons relevant to the characterization of the tested workflows.

Comparison of the tested manufacturing workflows showed a lower overall RMS deviation for DLP than for milling. Because additive and subtractive manufacturing technologies rely on different processing mechanisms, each technology requires a material system compatible with its respective manufacturing principle. In this study, we used a photopolymer resin for DLP fabrication and prepolymerized PMMA for milling. Therefore, this comparison was not intended to isolate the effect of material independently of the manufacturing technology, but rather to compare the occlusal surface geometric accuracy of two manufacturing workflow–material system combinations representative of clinical and laboratory practice. Consequently, findings related to the manufacturing method should be interpreted as reflecting the performance of the tested workflow–material combinations rather than the isolated effect of the manufacturing technology itself. Within this context, the findings are consistent with those of Al Sayed El Saaedi et al. [9], who reported lower surface deviations for 3D-printed complete denture teeth than for milled teeth, despite observing an accuracy advantage for milled denture bases. Wang et al. [5] emphasized that the geometric accuracy of digital complete dentures depends on the manufacturing system, geometry, material, and evaluation protocol; therefore, neither milling nor 3D printing can be considered universally superior under all conditions. Yoshidome et al. [18], Herpel et al. [19], and Schubert et al. [20] reported greater accuracy or adaptation for milled denture bases or trial dentures compared with printed alternatives; however, those studies evaluated broad denture-base or complete-denture surfaces rather than the complex occlusal morphology specifically investigated in the present study. Although additive manufacturing may be less constrained by bur diameter and tool accessibility when reproducing narrow grooves, fossae, and cusp transitions, it remains sensitive to layer thickness, printing orientation, support placement, and post-polymerization procedures [21].

Tooth- and geometry-specific effects reported in the literature also support cautious interpretation of the relative performance of manufacturing methods. Soeda et al. [8] showed that the accuracy of artificial teeth in CAD/CAM complete dentures varied by tooth type, and a subsequent study by the same group reported that the relative performance of manufacturing approaches could differ depending on the tooth evaluated [22]. These observations are consistent with the present finding that the manufacturing response was related not only to the production technology but also to the geometric configuration of the dental arch.

Segmented specimens had lower composite RMS values than one-piece specimens across all tooth sizes with both manufacturing methods. Three-segment tooth assemblies have also been investigated experimentally [23]. Shorter structures may undergo different cumulative dimensional changes during additive manufacturing and may alter tool accessibility and

toolpaths during milling [24]. These mechanisms were not measured directly and remain possible explanations rather than demonstrated causes. The significant manufacturing method × manufacturing configuration interaction indicates that the magnitude of the observed difference depended on the tested workflow. However, the comparison also incorporates differences in registration and aggregation, so the lower segmented RMS cannot be attributed exclusively to improved manufacturing trueness.

The three-segment design provides a manufacturing approach based on shorter anatomical units while retaining connected teeth within each unit. Its relevance for clinicians and laboratory technicians lies in investigating how such a configuration can preserve CAD-defined occlusal morphology and permit a defective segment to be remanufactured without repeating the entire tooth arch. The lower composite RMS observed across all tested sizes and both methods provides a quantitative rationale for further investigation of this configuration. Its effects on laboratory efficiency and clinical outcomes remain to be established. Segmented assemblies have been investigated previously [10,23]; Janice et al. [23] found no significant overall positional difference between bonded full-arch and three-segment assemblies, reinforcing the need to evaluate whether manufacturing-level findings persist after bonding.

Independent best-fit registration of each segment removes its rigid-body translation and rotation relative to the reference. In contrast, the one-piece arch retains the relative positions of all teeth during its single common alignment. A segment can therefore reproduce its local occlusal morphology closely while still being translated or rotated when assembled into the denture. Fixing the reference evaluation boundaries standardizes the surfaces examined but does not make these alignment constraints equivalent. In addition, the equal-weight quadratic mean of segment RMS values is not a pooled, point-weighted whole-arch RMS. The lower segmented outcome thus reflects the manufacturing configuration together with the assessment strategy and cannot establish superior absolute arch accuracy or quantify the net effect of segmentation after bonding.

The practical assessment of three-segment fabrication should consider both occlusal surface reproduction and assembly requirements. Three components require separate seating, stabilization, and bonding, followed by verification of their adaptation and occlusion. Socket fit, adhesive thickness, seating pressure, and movement during bonding or polymerization may introduce positional errors [10,17,23]. Such errors could offset the lower surface RMS observed before assembly, although their magnitude was not quantified here. Distinguishing manufacturing from assembly allows the present surface measurements to inform process development while defining the evidence needed for clinical implementation. Post-bonding accuracy, laboratory time, material consumption, and adjustment requirements should be compared before deciding whether routine adoption is warranted.

Tooth-set size also influenced surface geometric accuracy. Bonferroni-adjusted simple-effects comparisons following the significant three-way interaction showed that small, medium, and large tooth sets differed within each manufacturing method × manufacturing configuration combination, with RMS increasing progressively from small to large (a-c; $p < 0.001$). This pattern should be interpreted within the tested factor combinations. Moon et al. [25] reported a similar size-dependent pattern in DLP manufacturing, with greater RMS deviations in longer-span and full-arch interim restorations than in shorter structures. Increasing the geometric extent

of the fabricated structure may alter the accumulation of polymerization-related changes, support behavior, toolpath length, or accessibility to local geometric details.

The interaction pattern further supports evaluating digital manufacturing as a system rather than as a collection of isolated factors. Although the manufacturing method × tooth size interaction was not significant, the manufacturing method × manufacturing configuration, tooth size × manufacturing configuration, and three-way interactions were significant. Therefore, the effect of manufacturing configuration varied according to both manufacturing technology and tooth size. Previous studies have shown substantial differences in accuracy among desktop 3D printers. In addition, printing parameters and object geometry can influence dimensional accuracy [26,27]. The present findings extend this principle to complete denture teeth and indicate that tooth-set size and segmentation may jointly influence occlusal surface geometric accuracy.

Additional limitations should be considered. Only one DLP workflow, one milling workflow, one scanner, and one CAD tooth library were evaluated, limiting generalizability. The technology-specific photopolymer and PMMA systems mean that the method comparison represents the tested workflow–material combinations rather than an isolated effect of technology or material. Each arch or segment was scanned once, and scanning and registration repeatability were not quantified; their contribution to the measured deviations therefore cannot be separated from manufacturing error. This is relevant when interpreting differences of a few hundredths of a millimeter. Moreover, no functional loading, denture movement on supporting tissues, opposing-arch contacts, or patient outcomes were assessed. Together with independent alignment and equal-weight aggregation, these considerations define the scope of the manufacturing comparison and the further validation needed to relate the findings to the function of a completed denture.

Statistical significance should be distinguished from clinical importance. The differences in mean RMS between one-piece and segmented specimens were 0.0131–0.0368 mm (13.1–36.8 μm), calculated from the rounded means in Table 1. These are differences between surface-deviation summaries, not measurements of interocclusal gaps, contact interference, or displacement after assembly. A clinically meaningful threshold was not established for this RMS endpoint, and standardized effect sizes do not by themselves indicate a clinically perceptible benefit. An overall RMS value also does not identify the location or direction of individual occlusal discrepancies. Within this defined scope, the absolute RMS values and factor-specific patterns provide quantitative benchmarks for comparing occlusal morphology reproduction and guiding further manufacturing experiments. Their implications for occlusal adjustment and denture function require assessment after assembly and in clinical use.

Future studies should compare different photopolymer and PMMA systems within their respective manufacturing technologies and investigate printing, post-polymerization, and milling parameters. To determine the net value of segmentation, one-piece and segmented tooth assemblies should also be evaluated after standardized bonding using a common, base-referenced coordinate system that preserves intersegment translation and rotation, with comparable surface sampling and RMS weighting. Such studies should quantify assembly repeatability, positional deviations, laboratory time, cost, occlusal contacts, and adjustment requirements. Clinical investigations incorporating functional loading and patient-centered

outcomes are needed before a routine indication for three-segment fabrication can be established.

Conclusion

Within the tested workflow–material combinations and surface evaluation protocol, DLP specimens had lower occlusal RMS deviations than milled specimens, and independently aligned segmented specimens had lower composite RMS values than one-piece specimens. RMS increased from small to large tooth sets within each manufacturing method × manufacturing configuration combination. Significant interactions indicated that the magnitude of these differences depended on the combination of factors.

Together, the findings provide a quantitative basis for comparing the tested manufacturing workflows and investigating strategies that preserve planned occlusal morphology. Segmentation is a relevant variable for further protocol development, with its practical value depending on both surface reproduction and assembly accuracy. Independent segment registration excluded assembly-related translation and rotation, and the small RMS differences may have negligible clinical impact in vivo. Post-bonding and clinical validation are therefore needed before the measured surface differences can support recommendations for routine use.

Declaration of Generative AI and AI-assisted Technologies in the Writing Process

During the preparation of this work, the authors used ChatGPT (OpenAI) and Grammarly (Grammarly, Inc.) to improve the manuscript's language, readability, clarity, and organization. After using these tools, the authors reviewed and edited the content as needed and take full responsibility for the content of the article.

References

[1] E. Emami, R.F. de Souza, M. Kabawat, J.S. Feine, The impact of edentulism on oral and general health, Int. J. Dent. 2013 (2013) 498305. https://doi.org/10.1155/2013/498305.

[2] E. Hunter, L.D.M. Brito, P. Piyasena, E. Petrauskiene, N. Congdon, G. Tsakos, et al., Impact of edentulism on community-dwelling adults in low-income, middle-income and high-income countries: a systematic review, BMJ Open 14 (2024) e085479.

[3] A.S. Bidra, T.D. Taylor, J.R. Agar, Computer-aided technology for fabricating complete dentures: systematic review of historical background, current status, and future perspectives, J. Prosthet. Dent. 109 (2013) 361-366. https://doi.org/10.1016/S0022-3913(13)60318-2.

[4] C.J. Goodacre, A. Garbacea, W.P. Naylor, T. Daher, C.B. Marchack, J. Lowry, CAD/CAM fabricated complete dentures: concepts and clinical methods of obtaining required morphological data, J. Prosthet. Dent. 107 (2012) 34-46. https://doi.org/10.1016/S0022-3913(12)60015-8.

[5] C. Wang, Y.F. Shi, P.J. Xie, J.H. Wu, Accuracy of digital complete dentures: a systematic review of in vitro studies, J. Prosthet. Dent. 125 (2021) 249-256. https://doi.org/10.1016/j.prosdent.2020.01.004.

[6] M. Revilla-León, M. Özcan, Additive manufacturing technologies used for processing polymers: current status and potential application in prosthetic dentistry, J. Prosthodont. 28 (2019) 146-158. https://doi.org/10.1111/jopr.12801.

[7] N. Alharbi, D. Wismeijer, R.B. Osman, Additive manufacturing techniques in prosthodontics: where do we currently stand? A critical review, Int. J. Prosthodont. 30 (2017) 474–484. https://doi.org/10.11607/ijp.5079.

[8] Y. Soeda, M. Kanazawa, T. Hada, T. Arakida, M. Iwaki, S. Minakuchi, Trueness and precision of artificial teeth in CAD-CAM milled complete dentures with custom disks, J. Prosthet. Dent. 128 (2022) 695-701. https://doi.org/10.1016/j.prosdent.2020.12.049.

[9] T.M.A.S.E. Saaedi, Y.G. Thabet, M.E. Sabet, Evaluation of accuracy and position of milled and 3D-printed teeth in digital complete dentures, Int. J. Prosthodont. 36 (2023) 781-786. https://doi.org/10.11607/ijp.7984.

[10] R.M.A.M. Sallam, N.A. Metwally, M.M. Khamis, Evaluation of the occlusal trueness among 3-dimensionally printed CAD-CAM complete dentures with different socket designs and teeth splinting assemblies, BMC Oral Health 25 (2025) 626. https://doi.org/10.1186/s12903-025-05894-7.

[11] B.D. Tatlicioglu, E. Eroglu, K. Kiran, H. Ucak, Comparison of DLP and LCD 3D printing technologies: effects on denture base accuracy, weight, residual material, resin consumption, and production time, J. Dent. 165 (2026) 106270. https://doi.org/10.1016/j.jdent.2025.106270.

[12] L. Ciocca, M. Maltauro, V. Cimini, L. Breschi, A. Montanari, L. Anderlucci, et al., Analysis of the trueness and precision of complete denture bases manufactured using digital and analog technologies, J. Adv. Prosthodont. 15 (2023) 22-32. https://doi.org/10.4047/jap.2023.15.1.22.

[13] S. Namano, M. Kanazawa, K. Qi, B.N.H. Trang, K.P. Sone, M. Iwaki, Y. Komagamine, S. Minakuchi, Effects of support-structure design and postpolymerization protocols on dimensional changes in three-dimensionally printed complete dentures, J. Prosthet. Dent. 134 (2025) 190.e1-190.e9. https://doi.org/10.1016/j.prosdent.2025.03.003.

[14] P.J. Besl, N.D. McKay, A method for registration of 3-D shapes, IEEE Trans. Pattern Anal. Mach. Intell. 14 (1992) 239-256. https://doi.org/10.1109/34.121791.

[15] N. Sun, T. Bull, R. Austin, D. Bartlett, S. O'Toole, Quantifying error introduced by iterative closest point image registration, J. Dent. 142 (2024) 104863. https://doi.org/10.1016/j.jdent.2024.104863.

[16] S.J. Luck, A.X. Stewart, A.M. Simmons, M. Rhemtulla, Standardized Measurement Error: a universal metric of data quality for averaged event-related potentials, Psychophysiology 58 (2021) e13793. https://doi.org/10.1111/psyp.13793.

[17] Y.G. Thabet, M.E. Sabet, M.A. Nabil, T.M.A.S. El Saaedi, H.T. Mohamed, Assessment of tooth positions of printed complete dentures with different designs and tooth positioning techniques, J. Prosthodont. 33 (2024) 808-814. https://doi.org/10.1111/jopr.13769.

[18] K. Yoshidome, M. Torii, N. Kawamura, H. Shimpo, C. Ohkubo, Trueness and fitting accuracy of maxillary 3D printed complete dentures, J. Prosthodont. Res. 65 (2021) 559-564. https://doi.org/10.2186/jpr.JPR_D_20_00240.

[19] C. Herpel, A. Tasaka, S. Higuchi, D. Finke, R. Kühle, K. Odaka, et al., Accuracy of 3D printing compared with milling - a multi-center analysis of try-in dentures, J. Dent. 110 (2021) 103681. https://doi.org/10.1016/j.jdent.2021.103681.

[20] O. Schubert, D. Edelhoff, K.J. Erdelt, E. Nold, J.F. Güth, Accuracy of surface adaptation of complete denture bases fabricated using milling, material jetting, selective laser sintering, digital light processing, and conventional injection molding, Int. J. Comput. Dent. 25 (2022) 151-159. https://doi.org/10.3290/j.ijcd.b2588131.

[21] B.J. Goodacre, C.J. Goodacre, Additive manufacturing for complete denture fabrication: a narrative review, J. Prosthodont. 31 (2022) 47-51. https://doi.org/10.1111/jopr.13426.

[22] Y. Soeda, Y. Komagamine, M. Kanazawa, T. Hada, M. Iwaki, S. Minakuchi, Trueness and precision of artificial teeth in CAD-CAM milled complete dentures from custom disks with a milled recess, J. Prosthet. Dent. 132 (2024) 1014-1019. https://doi.org/10.1016/j.prosdent.2022.08.037.

[23] T.Z.H. Janice, C.A.P. Vanessa, C.K.S. Bryan, Y. Na, Accuracy of teeth positioning in bonded three-dimensionally printed complete dentures: an in vitro study, BMC Oral Health 26 (2026) 1785. https://doi.org/10.1186/s12903-026-09125-5.

[24] Y.G. Jeong, W.S. Lee, K.B. Lee, Accuracy evaluation of dental models manufactured by CAD/CAM milling method and 3D printing method, J. Adv. Prosthodont. 10 (2018) 245-251. https://doi.org/10.4047/jap.2018.10.3.245.

[25] W. Moon, S. Kim, B.S. Lim, Y.S. Park, R.J.Y. Kim, S.H. Chung, Dimensional accuracy evaluation of temporary dental restorations with different 3D printing systems, Materials 14 (2021) 1487. https://doi.org/10.3390/ma14061487.

[26] F.G. Mangano, O. Admakin, M. Bonacina, F. Biaggini, D. Farronato, H. Lerner, Accuracy of 6 desktop 3D printers in dentistry: a comparative in vitro study, Eur. J. Prosthodont. Restor. Dent. 28 (2020) 75-85. https://doi.org/10.1922/EJPRD_2050Mangano11.

[27] C. Arnold, L. Riß, J. Hey, R. Schweyen, Dimensional accuracy of different three-dimensional printing models as a function of varying the printing parameters, Materials 17 (2024) 3616. https://doi.org/10.3390/ma17143616.



Figure 1. Fabrication of complete denture teeth by subtractive manufacturing (milling).

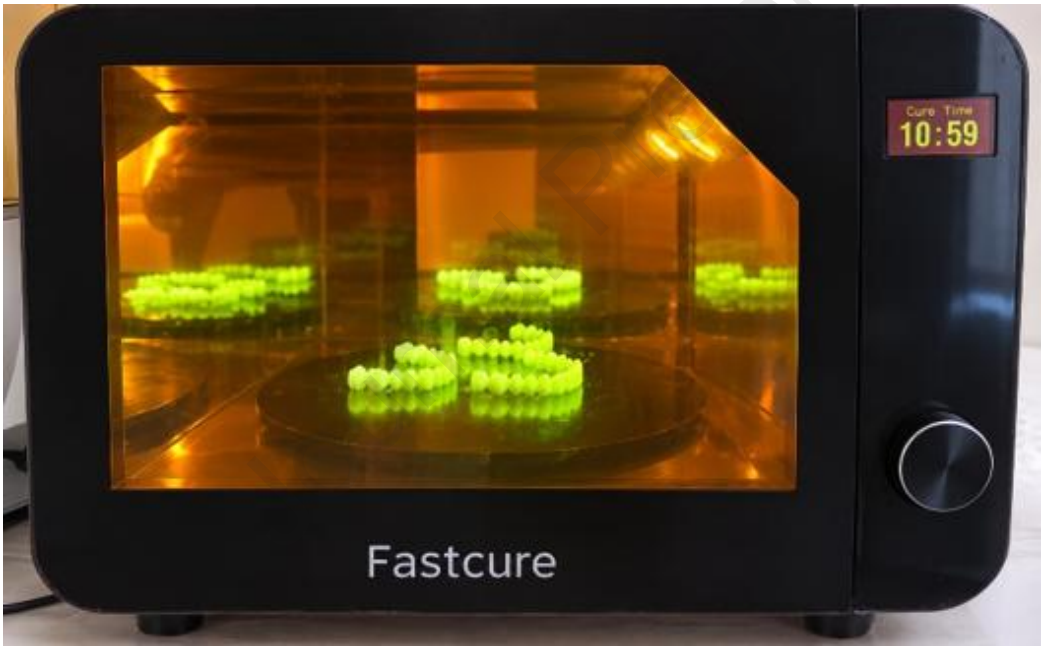


Figure 2. DLP additive manufacturing and post-polymerization.

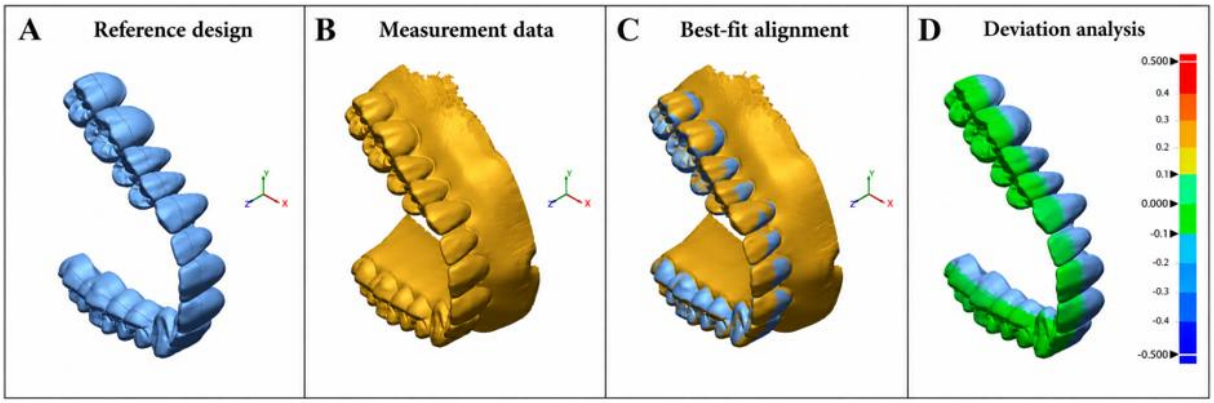


Figure 3. Workflow of scanning and deviation analysis: (A) reference design, (B) measurement data, (C) best-fit alignment, and (D) deviation analysis. Registration was restricted to the predefined occlusal surfaces and did not evaluate tooth position after assembly.

$$RMS_{\text{combined}} = \sqrt{\frac{RMS_{\text{anterior}}^2 + RMS_{\text{right}}^2 + RMS_{\text{left}}^2}{3}}$$

Figure 4. Calculation of the combined RMS value for segmented specimens using the equal-weight quadratic mean of the anterior, right posterior, and left posterior segment RMS values. Each segment was independently registered; the composite is not a measure of post-bonding arch positional accuracy.

Journal Pre-proof

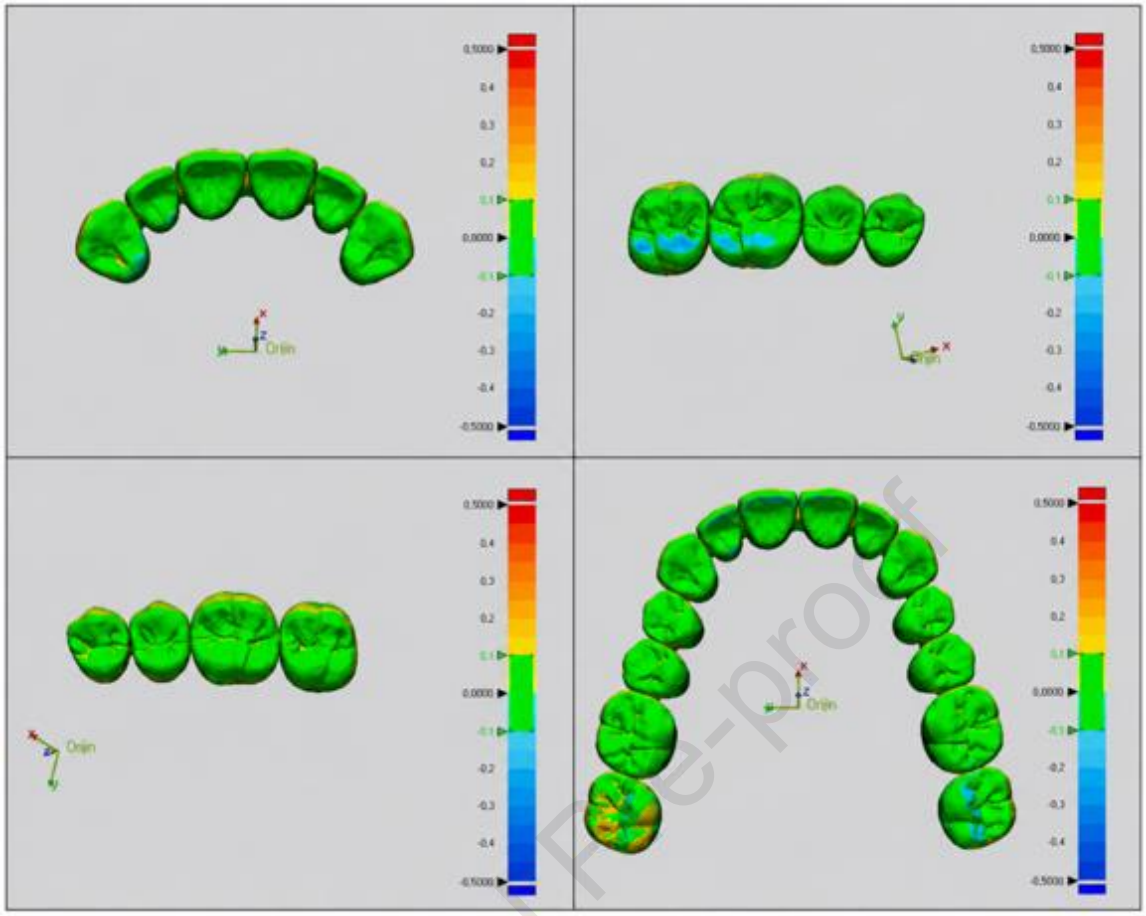


Figure 5. Color-coded occlusal surface deviation map of complete denture teeth fabricated by subtractive manufacturing (milling).

Journal Pre-proof

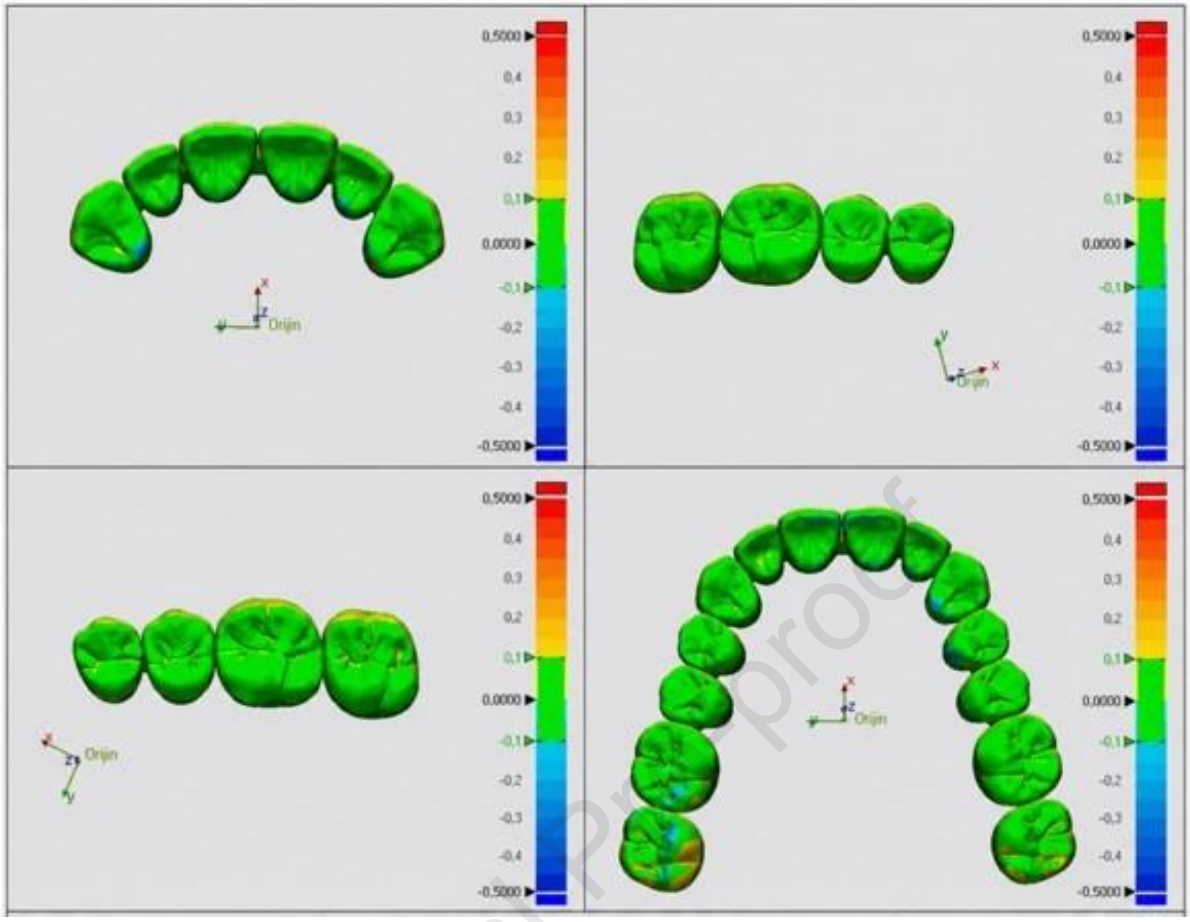


Figure 6. Color-coded occlusal surface deviation map of complete denture teeth fabricated by DLP additive manufacturing.

Journal Pre-proof

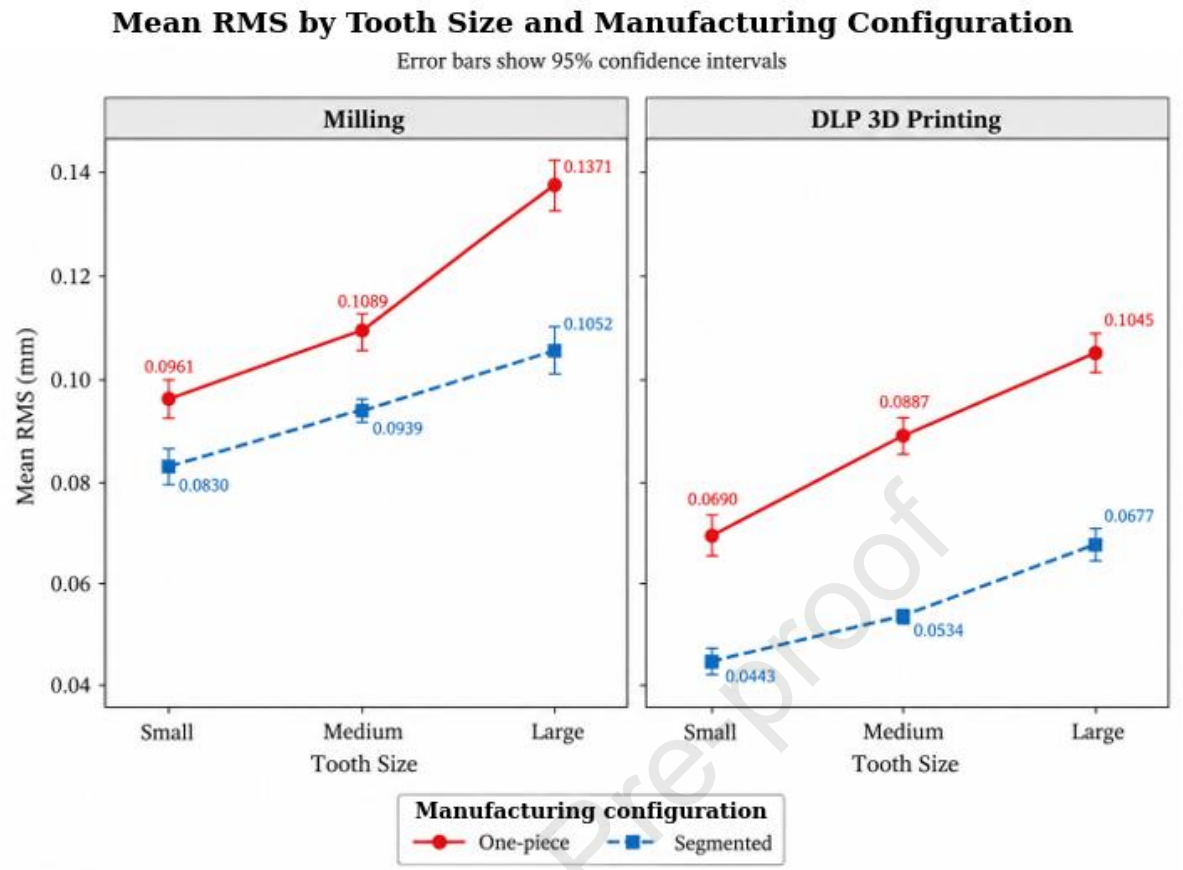


Figure 7. RMS values (mm) according to manufacturing method, manufacturing configuration, and tooth size. Error bars indicate 95% confidence intervals. One-piece values follow arch-level registration; segmented values are equal-weight composites following independent segment registration and represent surface morphology rather than the positional accuracy of a bonded assembly.

Journal Pre-proof

Journal Pre-proof

Declaration of interests

☒ The authors declare that they have no known competing financial interests or personal relationships that could have appeared to influence the work reported in this paper.

☐ The authors declare the following financial interests/personal relationships which may be considered as potential competing interests:

Journal Pre-proof